

Vibrational spectra and the structure of pure vitreous B_2O_3

F. L. Galeener, G. Lucovsky, and J. C. Mikkelsen, Jr.

Xerox Palo Alto Research Center, Palo Alto, California 94304

(Received 14 March 1980)

We report the polarized Raman spectra, the infrared reflectivity, and the infrared dielectric constant of vitreous B_2O_3 , for vibrational frequencies up to 1800 cm^{-1} . Longitudinal- and transverse-mode frequencies are identified. The dominant Raman line, at 808 cm^{-1} , is extremely narrow ($\sim 15\text{ cm}^{-1}$) and is highly polarized, with peak intensities in the ratio $HH/HV \sim 28$. (Here HH means that the incident and scattered electric vectors are parallel, while HV indicates that they are perpendicular.) The spectra are analyzed using a nearest-neighbor central-force network-dynamics model, and by comparison with data obtained from selected molecular species. The results favor a structural model containing a large fraction of boroxyl rings.

INTRODUCTION

Vitreous (v -) B_2O_3 is a transparent hygroscopic glass whose refractive index in the visible region ($n \sim 1.48$) is about the same as that of v - SiO_2 ($n \sim 1.46$). It has important technological applications as an additive in SiO_2 -based bulk glasses, fibers, and thin films. The material is especially interesting because of the suggestion by Goubeau and Keller¹ that v - B_2O_3 consists primarily of planar hexagonal B_3O_3 "boroxyl" rings, interconnected (at the boron sites) by bridging oxygen atoms or other small units. In their model, it is disorder in the interconnection of the boroxyl rings that accounts for the noncrystalline nature of the glass.

Although Krogh-Moe has shown that several properties of v - B_2O_3 are consistent with this model,² its uniqueness has not been proven and the existence of boroxyl rings has recently been seriously questioned.³ There is strong evidence from nuclear magnetic resonance (NMR) studies that each B atom is at the center of an equilateral triangle having an oxygen at each corner.⁴ Mozzi and Warren⁵ found that their x-ray radial distribution function (RDF) data were better fitted by a model in which most of these triangles were incorporated into boroxyl rings. More recently, however, Elliott³ has calculated RDF's from computer-generated structures and concluded that the x-ray data can be better understood by a continuous random network (CRN) of BO_3 triangles containing *no* planar boroxyl rings whatsoever. It is our conviction that study of the details of the vibrational spectra will prove more incisive than the RDF's for distinguishing between these models, although improved vibrational theories will be required to fully realize this potential.

In the present paper, we report the *polarized* Raman spectra,⁶ the infrared (ir) reflectivity,^{7,8} and the ir dielectric constants of anhydrous

v - B_2O_3 . The ir dielectric constants enable identification of certain Raman lines as transverse-optical (TO) or longitudinal-optical (LO) modes, while the Raman spectra show a richness of structure and polarization properties not previously reported. In the absence of a complete network theory, we compare our results with a nearest-neighbor central-force network model and with two models based on isolated molecular units: one intended to simulate the modes of BO_3 "triangles," and the other, boroxyl rings. These comparisons, coupled with arguments regarding the narrowness of the dominant Raman line lead us to favor the glass model involving large numbers of boroxyl rings.

EXPERIMENTAL DETAILS

Our samples were made from 99.999% B_2O_3 powder⁹ that was vacuum dehydrated at 150 to 180°C to reduce the water content in the glass product.¹⁰ The dehydrated powder was melted either in air in platinum-foil dishes (resulting in minimum strain upon cooling) or in evacuated carbon-coated fused-silica ampoules. Fining was easily achieved in 24 hours at 1000 to 1200°C . Furnace cooling of the melt produced better optical homogeneity than casting onto a cold surface. Rectangular parallelepipeds were cut, ground, polished (0.3 micron alumina), and sealed in individual silica ampoules where they were annealed for 24 h at $\sim 260^\circ\text{C}$ and stored. We found it essential to examine the samples between crossed polarizers, and to anneal out strain-induced optical rotations (which otherwise lead to partial scrambling of the polarized Raman spectra).

The Raman spectra were obtained in the 90° configuration with the samples still inside the ampoules. All samples showed broad luminescence bands in the vicinity of the Raman spectrum when excited by any of the lines from 514.5 to

457.9 nm that are available from an Ar⁺ ion laser. The data for ~1.5 W of excitation at 457.9 nm are shown in the present paper because at this wavelength the luminescence interfered very little with the Raman spectra. The scattered light was collected with *f*/1 optics and the photomultiplier pulses were counted for 10 sec at 5-cm⁻¹ intervals. A reference channel stabilized the effective laser intensity to one part in 3000.

The ir-reflectance spectra were obtained from samples removed from the ampoules and placed in a Perkin-Elmer Model 180 spectrometer flushed with dry nitrogen. Although the ir spectra may contain small errors due to hydration of the sample surface after polishing or transfer to the spectrometer, two reflectivity spectra taken in succession (without opening the spectrometer) showed no detectable change in reflectivity. In both the ir and Raman measurements, the spectral slit width was less than 5 cm⁻¹.

RAMAN AND INFRARED SPECTRA

Figure 1 shows the polarized (HH and HV) Raman spectra of *v*-B₂O₃. (Here, HH means that the incident and scattered electric vectors are parallel, while HV indicates that they are perpendicular.) The scattering strength relative to that of *v*-SiO₂ has been reported elsewhere.¹¹ The most prominent feature, at 808 cm⁻¹, has full width at half-maximum height of ~15 cm⁻¹ and is highly polarized, with peak intensities in the ratio HH/HV ~ 28. An even higher-intensity peak can be found at ~25 cm⁻¹, very near the laser line but off scale in Fig. 1. This line does not appear in the reduced Raman spectrum,¹² and therefore does not represent a peak in the density

of states, or in the vibrational matrix elements. It is a so-called Bose-Einstein peak and arises because the thermal population of vibrational states increases rapidly as the vibrational frequency tends to zero. A low-frequency peak with similar origin is seen in *v*-SiO₂ and *v*-GeO₂.¹³

Figure 2 depicts the ir reflectivity of *v*-B₂O₃ which shows much less structure than the Raman spectra.⁸

Figure 3 allows comparison of the reduced Raman spectra¹² I_{red}^p with the real (ϵ_1) and imaginary (ϵ_2) parts of the dielectric constant and with the energy-loss function, $\text{Im}(-1/\epsilon)$. The reduced Raman spectra are calculated from Fig. 1 as described in Ref. 12. The ϵ_1 , ϵ_2 , and $\text{Im}(-1/\epsilon)$ are calculated from Fig. 2 using Kramers-Kronig techniques. The frequencies of the principal features in these spectra are listed in Table I. Raman polarization ratios (HH/HV) can be computed directly from Figs. 3 or 1.

TO-LO ASSIGNMENTS

Certain vibrational modes in *v*-B₂O₃ exhibit large transverse-optical-longitudinal-optical (TO-LO) splittings. We shall discuss them with the help of Fig. 3, using the same approach as we have described earlier for TO-LO splittings in *v*-SiO₂,¹⁴ *v*-GeO₂,¹⁴ *v*-BeF₂,¹⁵ and *v*-As₂O₃.¹⁶ The solid vertical lines in Fig. 3 mark peaks in ϵ_2 , hence the frequencies of TO modes, while the dashed vertical lines mark peaks in $\text{Im}(-1/\epsilon)$, the positions of LO modes.

The lowest-frequency peak in ϵ_2 occurs at ~720 cm⁻¹. That there is no Raman-active peak at this frequency is perhaps not surprising, since we have also seen no discernible Raman line at

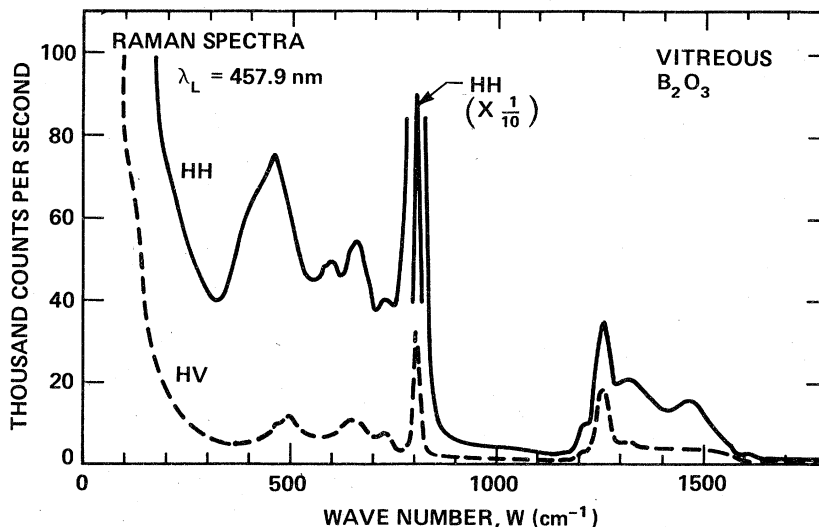


FIG. 1. Polarized Raman spectra of *v*-B₂O₃.

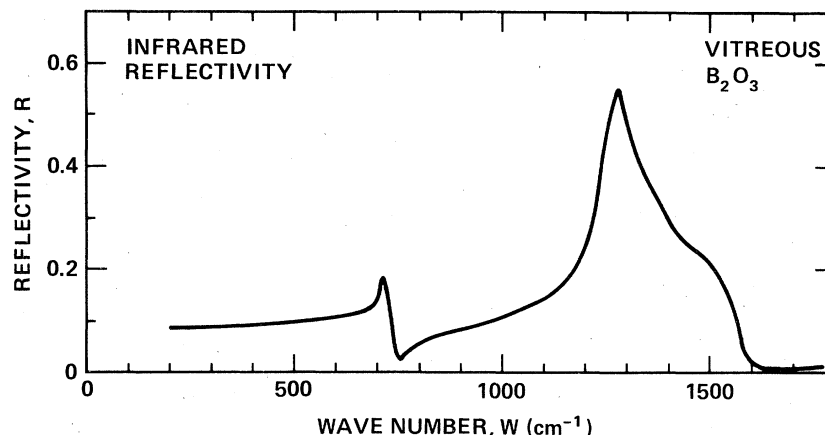


FIG. 2. ir reflectivity of v - B_2O_3 .

the lowest TO frequency in the tetrahedral glasses.^{14,15} Associated with this TO mode is an LO mode which peaks at about 740 cm^{-1} in the energy-loss function. We are reluctant to identify the Raman line at 740 cm^{-1} as an LO mode, since we see no reason for the LO form of this mode to have greater Raman activity than the TO form.

The highest-frequency peak in ϵ_2 occurs at $\sim 1260\text{ cm}^{-1}$, precisely in alignment with a Raman peak which we therefore identify as TO in character. There is also a peak in the energy-loss function at $\sim 1550\text{ cm}^{-1}$. The position of this LO mode corresponds to a shoulder in the Raman spectrum at about the same position, so we identify the shoulder as LO in character.

It is possible to interpret the Raman lines at 1335 and 1475 cm^{-1} as LO and TO, respectively, in analogy with the situation reported at high frequencies in v - BeF_2 (Ref. 15) and v - As_2O_3 .¹⁶ This assignment would then account for the shoulders seen in ϵ_2 and $\text{Im}(-1/\epsilon)$ in the region ~ 1250 to $\sim 1550\text{ cm}^{-1}$. According to this interpretation, there would be two high-frequency TO-LO pairs: 1260 - 1325 cm^{-1} and 1475 - 1550 cm^{-1} . If the "bare-mode" frequencies¹⁵ are near the LO modes, as appears to be the case^{15,17} in v - SiO_2 , v - GeO_2 , and v - BeF_2 , we would expect them to be approximately 1325 and 1550 cm^{-1} in v - B_2O_3 . (We will later call these frequencies ω_3 and ω_4 .)

SECOND-ORDER FEATURES

It is likely that the small feature at 1615 cm^{-1} is a harmonic of the main line seen at 808 cm^{-1} . Its frequency is twice that of the main line and its strength is down from the main line by a factor of ~ 700 , similar to the factors that have been demonstrated for second-order lines in several other glasses.¹⁸ The weak line at 1210 cm^{-1} seems too strong to be a harmonic of the

first-order line at 608 cm^{-1} . Second-order spectra due to the first-order features between 1200 and 1550 cm^{-1} are expected in the range 2400 to 3100 cm^{-1} . Sample luminescence in the latter region made it impossible for us to see the weak lines that are expected.

NEAREST-NEIGHBOR CENTRAL-FORCE CONTINUOUS RANDOM NETWORK ANALYSIS

Galeener¹⁷ has shown that the nearest-neighbor (NN) central-force *network* model derived by Sen and Thorpe¹⁹ for tetrahedral glasses can be applied with surprising accuracy to the interpretation of vibrational spectra of such glasses as v - SiO_2 , v - GeO_2 , and v - BeF_2 . More recently, Thorpe and Galeener²⁰ have extended the NN central-force calculations to cover several non-tetrahedral idealized *networks*, including ones appropriate to trigonal pyramidal glasses such as v - P_2O_5 and v - As_2O_3 . As a special case, they derive the following expressions for the four band edges of an idealized A_2X_3 CRN consisting of AX_3 planar triangles:

$$\omega_1^2 = (\alpha/m_X)(1 + \cos\theta), \quad (1)$$

$$\omega_2^2 = (\alpha/m_X)(1 - \cos\theta), \quad (2)$$

$$\omega_3^2 = \omega_1^2 + (3\alpha/2m_A), \quad (3)$$

$$\omega_4^2 = \omega_2^2 + (3\alpha/2m_A). \quad (4)$$

Here, ω_i are angular frequencies (rad/sec), α is the nearest-neighbor (A - X) central-force constant, and m_X and m_A are the masses of the X and A atoms.²¹ The angle θ is the A - X - A angle, assumed to be everywhere the same and the X - A - X angle has been taken to be 120° . Thus this model can be used to calculate the high-frequency vibrational response of the BO_3 -triangle model discussed in the Introduction.

A portion of the infinite network leading to Eqs. (1)-(4) is illustrated schematically in Fig. 4.

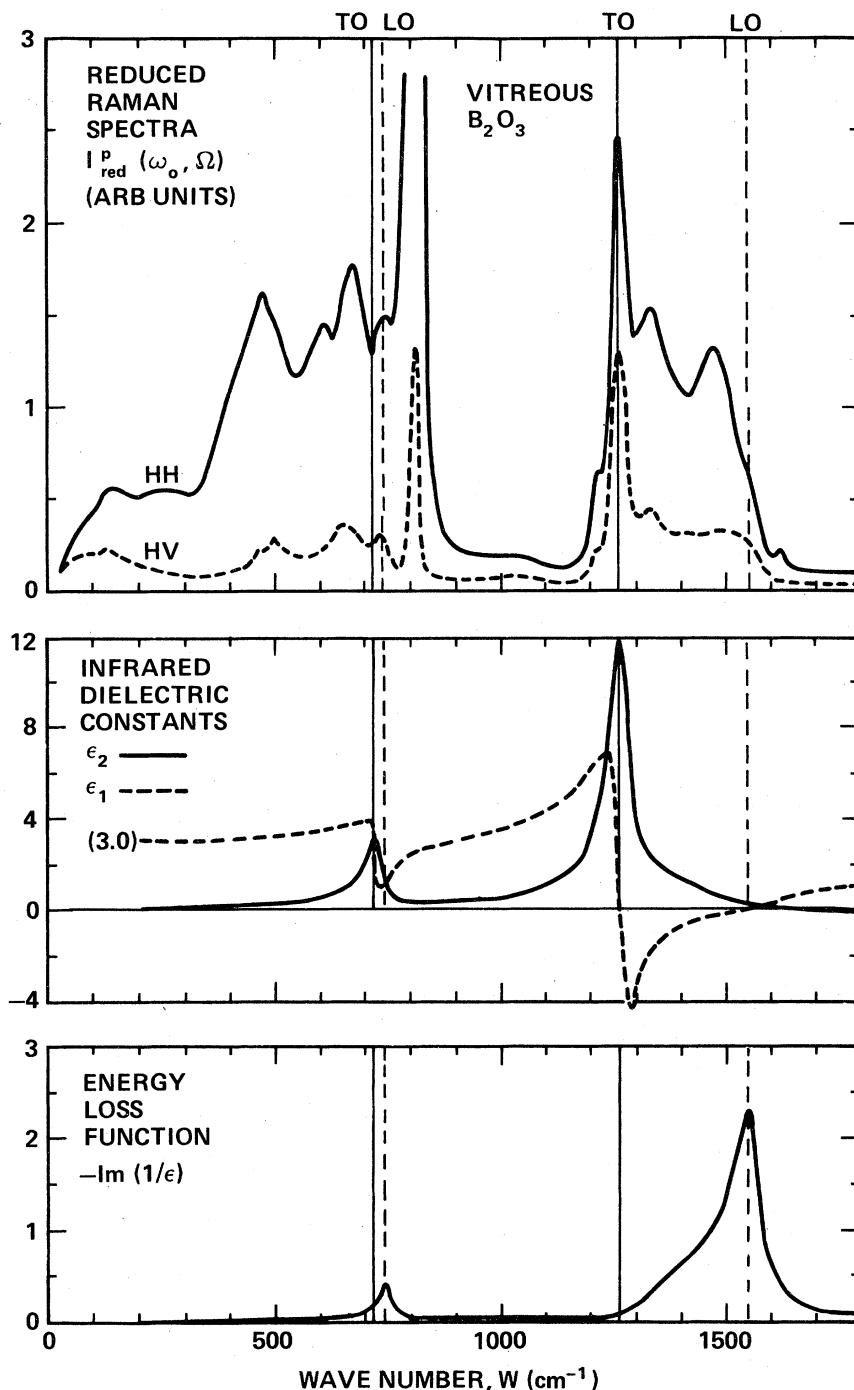


FIG. 3. Reduced Raman spectra, ir dielectric constants, and ir energy-loss function of v - B_2O_3 . Vertical lines indicate the position of peaks in ϵ_2 and $\text{Im}(-1/\epsilon)$.

Each A atom is at the *center* of an equilateral triangle formed by three X atoms; each X atom bridges two A atoms with the *same* intertriangular angle θ . Equations (1)–(4) are correct in the approximation of NN central forces for *any* distribution of dihedral angles. (A dihedral angle

specifies the orientation of an AX_3 triangle relative to an $A-X-A$ plane bridging the triangle to a neighboring A atom.)

Equations (1)–(4) are plotted as the solid lines in Fig. 5. The dashed lines are a *schematic* representation of the density of vibrational states,

TABLE I. Wave-number (cm^{-1}) positions of identifiable peaks in the vibrational spectra of $\nu\text{-B}_2\text{O}_3$ shown in Fig. 3. Positions are arranged in order of ascending frequency, and are segregated into a common horizontal row if within $\pm 8 \text{ cm}^{-1}$ of each other. The values given are good to at least $\pm 5 \text{ cm}^{-1}$.

$I_{\text{red}}^{\text{HH}}$	$I_{\text{red}}^{\text{HV}}$	ϵ_2	$\text{Im}(-1/\epsilon)$
145	130		
260			
470	470		
500	500		
610			
670	655		
		720 (TO)	
750	740		740 (LO)
808	808		
1030	1030		
1210	1210		
1260	1260	1260 (TO)	
1325 (LO ?)	1325		
	1400		
1475 (TO ?)	1490		
			1550 (LO)
1615			

with relative weights given in parentheses. The parameters used in these figures are those that we will deduce for $\nu\text{-B}_2\text{O}_3$, including $\theta(\text{B}_2\text{O}_3) \approx 120^\circ$. We will apply this picture to data taken from $\nu\text{-B}_2\text{O}_3$ in a manner exactly parallel to that employed for the tetrahedral glasses. For detailed description of the procedure, see Ref. 17.

Equations (3) and (4) can be solved for α and $\cos\theta$ in terms of the experimentally determined values $\omega_3 = \omega_3(\theta)$ and $\omega_4 = \omega_4(\theta)$:

$$\alpha = \frac{1}{2}(\omega_3^2 + \omega_4^2)m_X(1 + 3m_X/2m_A)^{-1}, \quad (5)$$

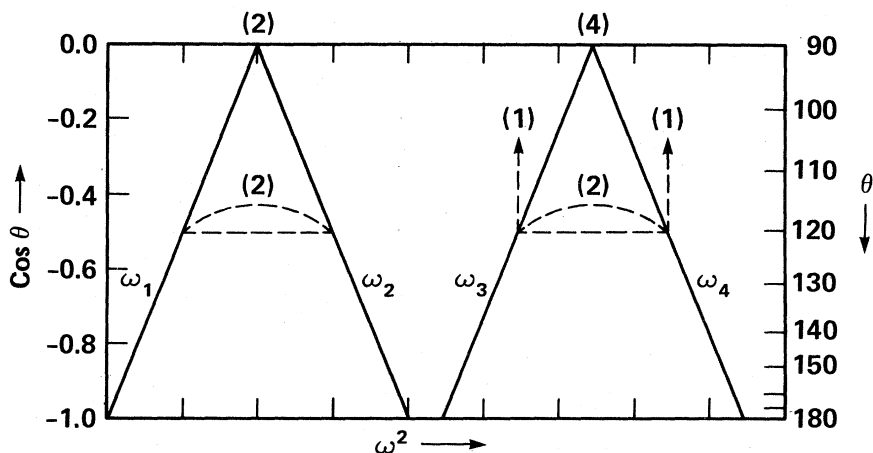


FIG. 5. Diagram of Eqs. (1)–(4) showing the dependence of band edges on intertriangular angle θ . The dashed lines are a schematic representation of the density of vibrational states at $\theta = 120^\circ$, with relative weights given in parentheses.

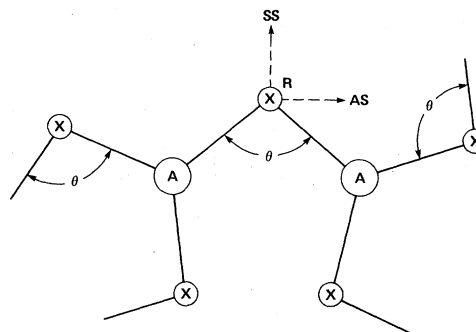


FIG. 4. Schematic diagram of the local order of an A_2X_3 glass based on AX_3 planar triangles connected together at the corners with common intertriangular angle θ .

$$\cos\theta = (\omega_3^2 - \omega_4^2)(\omega_3^2 + \omega_4^2)^{-1}(1 + 3m_X/2m_A). \quad (6)$$

To evaluate these for $\nu\text{-B}_2\text{O}_3$, we use $m_X = 16$ (for oxygen), $m_A = 10.8$ (for boron) and, following Galeener,¹⁷ we use the *LO* values of ω_3 and ω_4 (as the best available estimates of bare-mode frequencies).

The results are listed in Table II, where ω_3 and ω_4 are as shown, and α and θ follow from Eqs. (5) and (6). It is remarkable and probably fortuitous that θ is deduced to be 120° (the value it would have in a boroxyl ring). Having obtained α and θ , one can calculate ω_1 and ω_2 using Eqs. (1) and (2), with results shown in Table II. Study of the spectra in Fig. 3 reveals that neither ω_2 nor ω_1 corresponds to a prominent feature. This is to be contrasted with the fact that in the tetrahedral glasses, and in the trigonal glasses As_2S_3 and As_2Se_3 , ω_1 always corresponds well to the frequency of the dominant Raman peak, ω_R ,

TABLE II. Results of nearest-neighbor central-force analysis of vibrations in v - B_2O_3 . The central-force constant α (N/m) and intertriangular angle θ are deduced from the experimental LO frequencies ω_3 and ω_4 (cm^{-1}) using Eqs. (5) and (6). Equations (1) and (2) are then used to compute ω_1 and ω_2 , neither of which compares well with the observed frequency of the dominant Raman line, ω_R , in contrast to results obtained for tetrahedral glasses (Ref. 17). We conclude that the assumption of random dihedral angles is inadequate.

ω_3	ω_4	α	θ	ω_2	ω_1	ω_R
1325	1550	612	120	984	567	(808)

for reasons discussed elsewhere.^{17,22} We conclude that the NN central-force model for an idealized CRN of BO_3 triangles is inadequate.

The quantitative discrepancy between ω_1 and ω_R can probably be reduced by inclusion of noncentral forces; however, this improvement seems unlikely to lead to a sufficient number of new frequencies to account for the several Raman lines seen below $\omega_R = 808$ cm^{-1} . (It is known¹⁷ that inclusion of noncentral forces into the CRN model for the tetrahedral AX_2 glasses gives rise to only one more feature than is predicted by central forces only.) Thus we are led to relax a second restriction of the AX_3 -triangle model for v - B_2O_3 . We consider structural models in which the dihedral angles are *not* randomly distributed, and the boroxyl ring provides such a structure.

The boroxyl ring also provides a convenient explanation for the remarkable narrowness of the dominant Raman line at 808 cm^{-1} . This line has full width at half-maximum (FWHM) ΔW of about 15 cm^{-1} , an order of magnitude less than the 200 cm^{-1} FWHM of the dominant line in v - SiO_2 . If we assume that Eq. (1) is approximately correct¹⁷ for treating ω_R , we find that the 15- cm^{-1} FWHM implies a 1.5° spread in θ . If the dihedral angles are randomly distributed there seems to be no reason for this extremely narrow spread in θ . On the other hand the planar boroxyl ring ensures a special distribution of dihedral angles and a tight distribution of θ (at a value near 120°).

ISOLATED-MOLECULE ANALYSIS

The possible role of boroxyl rings is further discussed with the aid of Fig. 6, which compares the reduced Raman spectra of v - B_2O_3 with the reported vibrational frequencies of some related substances.

The vertical lines labeled (BF_3) are the observed vibrational frequencies of gaseous boron trifluoride²³ whose molecules, depicted in Fig. 6,

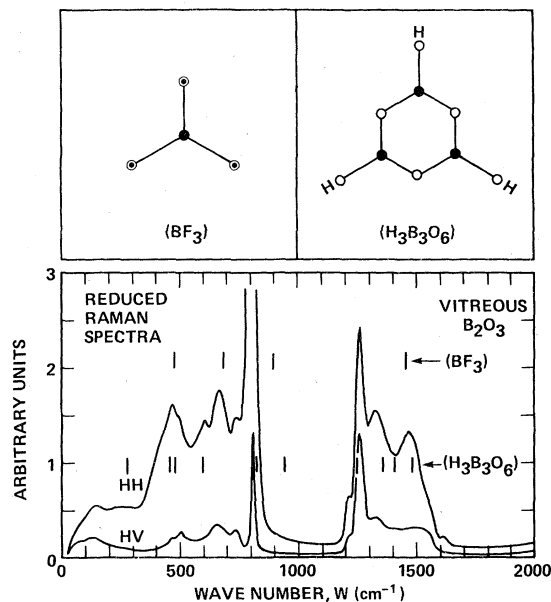


FIG. 6. Comparison of the reduced Raman spectrum of v - B_2O_3 with the observed frequencies of isolated molecules of BF_3 (planar triangles) and $H_3B_3O_6 = B_3O_3(OH)_3$ (planar boroxyl rings).

are planar and thus might be expected to relate to the frequencies of the planar BO_3 -triangle CRN model for v - B_2O_3 . The symmetric molecular mode at 888 cm^{-1} does not align well with the highly polarized 808- cm^{-1} peak in v - B_2O_3 spectrum. This discrepancy alone does not invalidate the BO_3 -triangle model since isolated BF_3 molecules cannot account for the substantial frequency shifts (and possible additional modes) that must arise in the glass, where each corner atom in a BO_3 triangle is shared by a neighboring BO_3 unit.²⁴ Also, the degree of polarization of the 808- cm^{-1} line is insufficient *ipso facto* to eliminate the triangle-network model. For example, the main Raman line of the tetrahedral CRN glass v - GeO_2 has HH/HV ~ 50 , and that of v - SiO_2 has HH/HV ~ 25 (see data in Ref. 14). To definitely eliminate the triangle-network model, we need a proper vibrational calculation, of the sort carried out for v - SiO_2 by Bell and co-workers.²⁵ In that case, however, no new bare modes were introduced above the number already predicted by an SiF_4 isolated-molecule model.¹³ For this reason it again seems unlikely that a "proper" calculation based on triangles connected with random dihedral angles will produce enough structure at low frequencies to approximate the spectra in Fig. 6.

We can estimate the effects of a particular kind of nonrandom dihedral angle distribution by looking at the frequencies of the orthorhombic form

of metaboric acid,²⁶ labeled ($H_3B_3O_6$) in Fig. 6. This crystalline substance consists of layers of planar molecules of the composition $B_3O_3(OH)_3$. These molecules are depicted in Fig. 6 where it is seen that three of the oxygen atoms are part of a boroxyl ring while the other three are connected to the boron atoms and terminated by hydrogen. These frequencies compare much better with the reduced Raman spectrum of $v\text{-}B_2O_3$ than do those of BF_3 . The most encouraging correspondences are to the $v\text{-}B_2O_3$ lines at HH cm^{-1} values 470, 500, 610, 1475, and, especially, at 808 and 1260. It is reasonable to interpret the excellence of these correspondences as vibrational evidence for large numbers of boroxyl rings in $v\text{-}B_2O_3$.²⁷

There are clearly some discrepancies between the frequencies of ($H_3B_3O_6$) and $v\text{-}B_2O_3$ and these may add additional information about the structure of the glass. The most obvious difference is the absence of a line corresponding to the $670\text{-}cm^{-1}$ peak in the reduced Raman spectrum. This peak may arise in the glass from the coupling of B_3O_3 rings by bridging oxygen atoms, or larger units, an interaction that is eliminated in ($H_3B_3O_6$) by the hydrogen terminators. For example, we note that BF_3 has a mode very near $670\text{-}cm^{-1}$. In the isolated molecule this mode is *not* Raman active; however, Raman activity might well be induced in the disordered environment of the glass. In that case, the $670\text{-}cm^{-1}$ line would indicate the presence of a substantial number of BO_3 units that are *not* incorporated into boroxyl rings. The resultant mixture of boroxyl rings and triangular BO_3 units is consistent with the model put forth by Mozzi and Warren⁵ as best explaining their x-ray RDF data.

BOROXYL RINGS IN THIN-FILM B_2O_3

It is worthwhile to note that we have seen the $808\text{-}cm^{-1}$ Raman line in a $1\text{-}\mu\text{m}$ -thick film of amorphous B_2O_3 .²⁸ This film was fabricated by Dr. J. Wong of the General Electric Corporation using techniques of chemical vapor deposition (CVD).⁸ The line was observed in the HH configuration at precisely the same position and with the same linewidth as in the bulk material. The HV spectrum was too weak to detect. If the line at $808\text{-}cm^{-1}$ is indeed the signature of boroxyl rings, then these rings also exist in CVD thin-film material.

SUMMARY

We have reported the polarized Raman spectra and the infrared spectra of $v\text{-}B_2O_3$ taken at room

temperature. These have been used to calculate the reduced HH and HV Raman spectra, as well as infrared values of the real and imaginary parts of the complex dielectric constant $\epsilon = \epsilon_1 + i\epsilon_2$, and the infrared energy-loss function $\text{Im}(-1/\epsilon)$. The computed spectra have been used to identify certain modes as TO-LO split pairs. The upper two LO-mode frequencies have been used in a nearest-neighbor central-force analysis to deduce a central-force constant $\alpha = 612\text{ N/m}$ and a B-O-B angle θ of about 120° . The fact that this analysis does *not* deduce an accurate value for the frequency of the dominant Raman line ($808\text{-}cm^{-1}$) suggests inadequacies associated with the assumption of random dihedral angles. Use of the central-force model to investigate the extreme narrowness of the $808\text{-}cm^{-1}$ line suggests a spread in θ of only $\sim 1.5^\circ$. The requirements of nonrandom dihedral angle distribution and very narrow spread in θ are met quite naturally by the boroxyl-ring structure, already suggested by others. Comparison of the Raman spectra with vibrational frequencies reported for "triangular" molecules of BF_3 and "boroxyl ring" molecules of $H_3B_3O_6$ also provides evidence for the presence of boroxyl rings, as well as some other element(s) of structure which may be BO_3 triangles that are not part of boroxyl rings. Thus, our vibrational studies support the kind of model set forth by Mozzi and Warren,⁵ involving a mixture of B_3O_3 boroxyl rings and BO_3 triangles; they are inconsistent with the implication of Elliott's recent x-ray analysis³ that boroxyl rings do not exist in $v\text{-}B_2O_3$.

Further work is suggested in several areas. Experimentally it is desirable to obtain a convincing estimate of the relative concentrations of boroxyl rings and connecting units (presumably BO_3 triangles). Inelastic neutron scattering data are needed to complete the data desirable for a definitive vibrational analysis. Theoretically, it is important to extend the nearest-neighbor central-force model to account for *closed* rings, and this requires treatment of noncentral forces. It is also desirable to have a realistic large-cluster calculation for both the triangle and boroxyl-ring network models, of the type pioneered for tetrahedral glasses by Bell and co-workers.

ACKNOWLEDGMENTS

The authors are grateful to Mr. W. J. Mosby for major assistance in acquiring the Raman spectra, to R. H. Geils for helpful discussions during the early stages of sample preparation, and to Dr. J. Wong for preparing the thin-film material.

- ¹J. Goubeau and H. Z. Keller, *Inorg. Chem.* **272**, 303 (1953).
- ²J. Krogh-Moe, *J. Non-Cryst. Solids* **1**, 269 (1969).
- ³See, e.g., S. R. Elliott, *Philos. Mag.* **B37**, 435 (1978).
- ⁴A. H. Silver and P. J. Bray, *J. Phys. Chem.* **29**, 984 (1958); S. E. Svanson, E. Forslind, and J. Krogh-Moe, *ibid.* **66**, 174 (1962).
- ⁵R. L. Mozzi and B. E. Warren, *J. Appl. Crystallogr.* **3**, 251 (1970).
- ⁶For a recent example of an *unpolarized* spectrum, see G. E. Walrafen, S. R. Samanta, and P. N. Krishnan, *J. Chem. Phys.* **72**, 113 (1980); also, see W. L. Konijnendijk and J. M. Stevels, *J. Non-Cryst. Solids* **18**, 307 (1975).
- ⁷For earlier ir reflectivity, see N. F. Borrelli, B. D. McSwain, and Gouq-Jen Su, *Phys. Chem. Glasses* **4**, 11 (1963).
- ⁸Somewhat more detail can be discerned in ir-transmission data. See, e.g., A. S. Tenney and J. Wong, *J. Chem. Phys.* **56**, 5516 (1972).
- ⁹Alfa-Ventron, 152 Andover Street, Danvers, MA 01923.
- ¹⁰Suggested to us by R. H. Doremus, private communication.
- ¹¹F. L. Galeener, J. C. Mikkelsen, R. H. Geils, and W. J. Mosby, *Appl. Phys. Lett.* **32**, 34 (1978).
- ¹²The reduced Raman spectrum is derived and defined in F. L. Galeener and P. N. Sen, *Phys. Rev. B* **17**, 1928 (1978).
- ¹³F. L. Galeener, in *Lattice Dynamics*, edited by M. Balkanski (Flammarion, Paris, 1978), p. 345.
- ¹⁴F. L. Galeener and G. Lucovsky, *Phys. Rev. Lett.* **37**, 1474 (1976).
- ¹⁵F. L. Galeener, G. Lucovsky, and R. H. Geils, *Solid State Commun.* **25**, 405 (1978).
- ¹⁶F. L. Galeener, G. Lucovsky, and R. H. Geils, *Phys. Rev. B* **19**, 4251 (1979).
- ¹⁷F. L. Galeener, *Phys. Rev. B* **19**, 4292 (1979); and *Bull. Am. Phys. Soc.* **23**, 338 (1978).
- ¹⁸F. L. Galeener and G. Lucovsky, in *Light Scattering in Solids*, edited by M. Balkanski, R. C. C. Leite, and S. P. S. Porto (Flammarion, Paris, 1976), p. 641; also, F. L. Galeener and G. Lucovsky, in *Structure and Properties of Non-Crystalline Semiconductors*, edited by B. T. Kolomiets (Nauka, Leningrad, 1976), p. 305.
- ¹⁹P. N. Sen and M. F. Thorpe, *Phys. Rev. B* **15**, 4030 (1977).
- ²⁰M. F. Thorpe and F. L. Galeener, *Bull. Am. Phys. Soc.* **24**, 457 (1979); and *Phys. Rev. B* **22**, 3078 (1980).
- ²¹All equations in this paper remain true if we replace ω by the wave-number value W (cm^{-1}) of the frequency, m by the atomic weight M of the atom, and α by $\alpha/0.0593$, where $\alpha = \alpha$ (dyn/cm) = $10^3\alpha$ (N/m). For example, Eq. (1) becomes $W_1^2 = [10^3\alpha(N/m)/0.0593M](1 + \cos\theta)$.
- ²²R. M. Martin and F. L. Galeener, *Bull. Am. Phys. Soc.* **24**, 495 (1979); and *Phys. Rev. B*, in press.
- ²³K. Nakamoto, *Infrared Spectra of Inorganic and Coordination Compounds* (Wiley, New York, 1973), p. 97.
- ²⁴In analogy with the case for tetrahedral glasses, as discussed in Ref. 13.
- ²⁵For review of the results of a large cluster calculation, see R. J. Bell, in *Methods in Computational Physics*, edited by G. Gilat (Academic, New York, 1976), p. 215.
- ²⁶L. A. Kristiansen and J. Krogh-Moe, *Phys. Chem. Glasses* **9**, 96 (1968).
- ²⁷To achieve a structural determination from vibrational studies, it is not enough to show that a model containing boroxyl rings can approximate the vibrational spectra; one must show that other reasonable models *cannot*. An experimental approach to this problem was recently published by J. P. Bronswijk and E. Strijks, *J. Non-Cryst. Solids* **24**, 145 (1977). They show that a form of crystalline B_2O_3 having no boroxyl rings also has no Raman line at 808 cm^{-1} . Even this is not conclusive, since the material is an array of chains of BO_3 triangles whose interconnections are certainly not the same as in a CRN of triangles.
- ²⁸F. L. Galeener and J. Wong (unpublished).